Intracortical human recordings reveal intensity coding for the pain of others in the insula

Efe Soyman,[1,2,†] Rune Bruls,[1,†] Kalliopi Ioumpa,[1,†] Laura Müller-Pinzler,[3] Selene Gallo,[1,4] Elisabeth C.W. van Straaten,[5] Matthew W. Self,[6] Judith C. Peters,[6,7,8] Jessy K. Possel,[6] Yoshiyuki Onuki,[9] Johannes C. Baayen,[10] Sander Idema,[10] Christian Keysers[1,11,‡] and Valeria Gazzola[1,11,‡]

[†,‡]**These authors contributed equally to this work.**

Author affiliations:
1 Social Brain Lab, Netherlands Institute for Neuroscience, Royal Netherlands Academy of Art and Sciences, 1105 BA, Amsterdam, the Netherlands
2 Social Cognitive and Affective Neuroscience Lab, Kadir Has University, Cibali 34083, Fatih, Istanbul, Turkey
3 Social Neuroscience Lab, Department of Psychiatry and Psychotherapy, University of Lübeck, 23562, Lübeck, Germany
4 Department of Psychiatry, Amsterdam University Medical Center, 1105 AZ, Amsterdam, the Netherlands
5 Department of Neurology and Clinical Neurophysiology, Amsterdam UMC, Vrije Universiteit Amsterdam, 1117 HV, Amsterdam, the Netherlands
6 Department of Vision and Cognition, Netherlands Institute of Neuroscience, Royal Netherlands Academy of Art and Sciences, 1105 BA, Amsterdam, the Netherlands
7 Department of Cognitive Neuroscience, Faculty of Psychology and Neuroscience, Maastricht University, 6229 EV, Maastricht, the Netherlands
8 Maastricht Brain Imaging Center (M-BIC), Maastricht University, 6229 EV, Maastricht, the Netherlands
9 Department of Neurosurgery, Jichi Medical University, 329-0498, Tochigi, Japan
10 Department of Neurosurgery, location VUmc, Amsterdam University Medical Center, 1117 HV, Amsterdam, The Netherlands
11 Brain and Cognition, Department of Psychology, University of Amsterdam, 1018 WS, Amsterdam, The Netherlands

Correspondence to: Valeria Gazzola or Christian Keysers
Netherlands Institute for Neuroscience, Meibergdreef 47, 1105 BA Amsterdam, NL
v.gazzola@nin.knaw.nl or c.keysers@nin.knaw.nl

Running title: Perceived intensity coding in the insula

Keywords: Insula; Pain; Empathy; Intracortical EEG; Broadband Gamma

Abbreviations: BA44/45=Brodmann Area 44/45; BBP=Broad-Band Power 20-190 Hz; BF_{10}=Bayes Factor in favour of a two-tailed alternative hypothesis; BF_{01}=Bayes Factor in favour of the null hypothesis relative to the two-tailed alternative hypothesis; BF_{+0}=Bayes Factor in favour of a one-tailed alternative hypothesis; Fp1=Frontal pole region 1; iEEG=intracortical EEG; MNI=Montreal Neurological Institute coordinate system; OP8/9=Frontal Opercular regions 8 and 9; p_1=one-tailed p value; p_2=two-tailed p value; r_K=Kendall's Tau correlation coefficient.; r_P=Pearson's correlation coefficient; r_S=Spearman's rank correlation coefficient

Abstract

Based on neuroimaging data, the insula is considered important for people to empathize with the pain of others, whether that pain is perceived through facial expressions or the sight of limbs in painful situations. Here we present the first report of intracortical electroencephalographic (iEEG) recordings from the insulae collected while 7 presurgical epilepsy patients rated the intensity of a woman's painful experiences viewed in movies. In two separate conditions, pain was deduced from seeing facial expressions or a hand being slapped by a belt. We found that broadband activity in the 20-190 Hz range correlated with the trial-by-trial perceived intensity in the insula for both types of stimuli. Using microwires at the tip of a selection of the electrodes, we additionally isolated 8 insular neurons with spiking that correlated with perceived intensity. Within the insula, we found a patchwork of locations with differing selectivities within our stimulus set, some representing intensity only for facial expressions, others only for the hand being hit, and others for both. That we found some locations with intensity coding only for faces, and others only for hand across simultaneously recorded locations suggests that insular activity while witnessing the pain of others cannot be entirely reduced to a univariate salience representation. Psychophysics and the temporal properties of our signals indicate that the timing of responses encoding intensity for the sight of the hand being hit are best explained by kinematic information; the timing of those encoding intensity for the facial expressions are best explained by shape information in the face. In particular, the furrowing of the eyebrows and the narrowing of the eyes of the protagonist in the movies suffice to predict both the rating of and the timing of the neuronal response to the facial expressions. Comparing the broadband activity in the iEEG signal with spiking activity and an fMRI experiment with similar stimuli revealed a consistent spatial organization for the representation of intensity from our hand stimuli, with stronger intensity representation more anteriorly and around neurons with intensity coding. In contrast, for the facial expressions, we found that the activity at the three levels of measurement do not coincide, suggesting a more disorganized representation. Together, our intracortical recordings indicate that the insula encodes, in a partially intermixed layout, both static and dynamic cues from different body parts that reflect the intensity of pain experienced by others.

Introduction

Sharing the distress of others is central to empathy. fMRI shows a number of brain regions involved in the experience of pain also increase their activity while participants perceive the pain of others, including the cingulate cortex, the insula, and the somatosensory cortices.[1–4] Across humans, primates, and rodents, lesions in these regions impair the perception and the sharing of others' emotions.[5] Directly recording electrical signals from these regions in humans would complement the more indirect fMRI measurements and sharpen our understanding of how these regions represent the intensity of other people's pain.

For the anterior cingulate we have intracortical recordings: Hutchison *et al.*[6] documented a single neuron in epileptic patients that responded to the sight of a finger being pin-pricked with increased firing rate, and a recent rodent study revealed that cingulate neurons responding to pain experience have responses that increase with the intensity of the pain experienced by another rat.[7] In contrast, although the insula is central in the neuroimaging literature on empathy and shows increases of BOLD signal for watching painful compared to non-painful social stimuli,[1,3,4,8–11] we still lack such intracortical recordings while individuals witness the pain of others. Intracortical EEG (iEEG) has been recorded in the insula during the self-experience of pain,[12] and the insula and adjacent SII are the only cortical regions where iEEG electrode stimulation can induce painful sensations,[13,14] but to our knowledge there are no published studies recording from insular electrodes while patients witness the pain of others.

To characterize the insula's electrophysiological responses to the pain of others, we recorded iEEG in 7 epileptic patients during presurgical exploration, while participants rated the pain they perceived another person in a video to experience. All these patients had macro-contacts in their insulae that yielded local field potentials (LFP, Fig. 1b). Three, additionally, had micro-wires at the tip of some electrodes to record from isolated insular neurons. Based on fMRI studies showing increased activity in the insula for more painful stimuli, we expected increases in power in higher LFP frequencies and spike counts for more intense stimuli, and used one-tailed testing unless specified otherwise. Our stimuli included two ways in which pain is perceived in others (Fig. 1a). Half the stimuli (Face videos) showed a female receiving electroshocks on the hand and expressing pain through facial expressions (furrowing eyebrows and tightening eyes). The other half (Hand videos) showed the protagonist's hand slapped by a leather belt, and pain intensity had to be deduced from the movements of the belt and the hand. In both cases, movies, rather than static images, were chosen to provide richer and more ecological stimuli and to provide information about the temporal dynamics with which such movies are represented in a field still dominated by the presentation of static images.[15,16] We used these two classes of stimuli, because both tap into the visual perception of other people's pain, and we start to understand that they do so through dissociable routes.[2–4] For instance, the hand stimuli depend on the hand region of the somatosensory cortex,[17] while facial expressions depend on the ventral somatosensory cortex and the insula.[18–20]

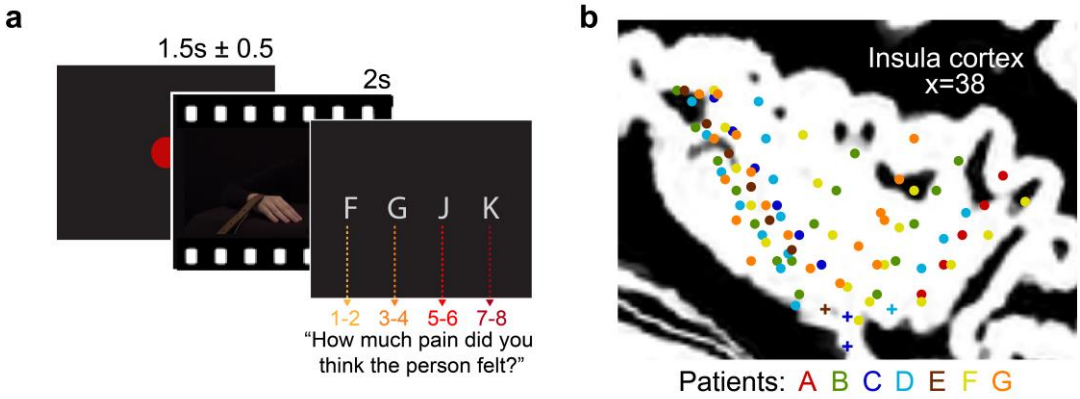

Figure 1 Experimental design and recording site locations. **(a)** Single trial structure diagram. For the Face videos, the first second of each movie showed a neutral facial expression, the second, the facial reaction to the shock. For the Hand videos, the movie started with the belt resting on the hand. The first second showed the belt lifting and coming down again, to hit the hand at the 1 s mark exactly. The hand then reacted to the force of the belt. Both the slap and the shock delivery happened in the middle of the movies, splitting them into a 1 s neutral and a 1 s pain period. After the presentation of each video, patients expressed their choice at their pace using the keyboard keys f, g, j, k for pain intensities 1-2, 3-4, 5-6, 7-8, respectively. ITI started with participant's response. **(b)** Position (i.e. midpoint between two adjacent electrodes) of the 85 bipolar recording sites shown as dots and of the microwire locations shown as plusses, color coded by patient. Data from the two hemispheres and all latero-medial coordinates are projected here onto a single sagittal slice of the insula taken at X=38 from the brain of one of the patients. For a list of all MNI coordinates, see Supplementary Table 2.

Materials and methods

Patients and electrodes

Depth electrode recordings were collected from nine epileptic volunteers, admitted at the Amsterdam UMC to localize seizure origin. Patients received initial study information from the neurosurgeon and provided informed consent to the experimenter before the surgery occurred. Our single session experiment started on average 4 days after surgery (std=1.89 days). Two patients were excluded from the analyses due to poor behavioral performance (Supplementary Note 1), and seven were included (4 females, 34.3±9 years). The study was approved by the medical ethical committee of the Vrije University Medical Center (protocol 2016/037) and each patient signed a written informed consent according to the Declaration of Helsinki. There was no indication of epileptic onset in electrode locations used in our analyses (Supplementary Note 2). Patients were implanted with Behnke-Fried depth electrodes[21] (Ad-Tech Medical Instrument Corporation) targeted at the right or left, anterior or posterior insula.

Video pain rating task

The 2 s videos were generated as in Gallo *et al.*[17] and showed a Caucasian female receiving either electrical shocks to the hand (reaction conveyed by the facial expression only; Face condition) or a slap with a belt to the hand (reaction conveyed by the hand only; Hand condition). Hence the location of the noxious stimulation was maintained across conditions (dorsum of the left hand), but the cues through which participants could deduce the painfulness differed. All videos started with 1 s of baseline: neutral facial expression for Face and static hand for Hand stimuli. Movies were cut, so that evidence of pain started at 1 s (Fig. 1a). Before the experiment, participants were instructed to rate pain intensity ("How much pain do you think the person felt?") on a scale from 0 (no pain at all) to 10 (the worst imaginable pain). They were informed that during video recording stimulations in the 9-10

range were never used. Participants had to rate pain intensity after each video at their own pace, using 4 keyboards-keys (Fig. 1a). Only the relevant keys were presented on the screen, intensities were not indicated. Patients watched each of the 60 videos (30 Hand, 30 Face) twice in fully randomized fashion with a random interval of 1.5±0.5 s.

Preprocessing of LFP signals

To reduce artefacts and extract local signals, iEEG macro-contact recordings were digitally re-referenced in a bipolar layout (Supplementary Fig. 2). This generated 85 bipolar recordings from 102 contacts in the insula, with patients having between 5 and 19 bipolar channels (Fig. 1b, Supplementary Table 2). Re-referencing attenuated 50 Hz noise sufficiently to omit digital filters that distort data. Continuous recordings were separated into trials of 4 s: 1 s pre-movie baseline, 2 s video, and 1 s post-movie. Trials were visually checked for ground failure and amplitude saturation (none was detected), downsampled to 400 Hz, and detrended.

Time-frequency decomposition of LFP signals

A sliding window Hanning taper based approach was used for each trial with the following parameters: frequencies from 1 to 200 Hz in steps of 1 Hz; time points from -1 s (relative to movie onset) to 3 s in steps of 0.0025 s; and for each frequency, a single sliding Hanning taper window with the duration of 8 cycles (maximum=1 s; minimum=0.1 s). Trials were expressed as % power change relative to baseline (-1 s to 0 s) separately for each frequency: $y(t)=100*(P(t)-P_0)/P_0$, with P_0=average of baseline. Points with y(t) ±10 standard deviations from the mean of the other trials were excluded to not reject entire trials, but only outlier time-frequency points in some trials (rejections were rare, mean rejected time-frequency points=0.0032±0.0035%).

General statistical approach and intensity coding

Our core question is how the insula codes perceived intensity. Supplementary Note 4 describes our statistical approach in detail. Briefly, we consider a bipolar channel to show *intensity coding*, if its trial-by-trial power variations correlate positively with the variation in pain intensity reported by the patient. We always recoded the 1-2, 3-4, 5-6, 7-8 rating options as 1, 2, 3, 4. For each bipolar recording, we then calculated the Spearman's rank correlations (due to the ordinal nature of intensity ratings) between the patient's intensity rating and power estimate over all trials for each time-frequency intersection separately, or within a certain power-band. A one-sample t-test was used to test whether the average correlation over the 85 bipolar recordings differed from 0. Where Shapiro-Wilk tests suggest deviations from normality, non-parametric t-tests were used as indicated by W (Wilcoxon signed rank) or U (Mann-Whitney U). Additionally, where evidence for the absence of an effect is relevant, we provide Bayes Factors that quantify the relative evidence for H_1 and H_0 (BF_{10}), or for a one-tailed H_+ vs H_0 (BF_{+0}), and use BF<⅓ as the critical bound for evidence of absence as detailed in Keysers *et al.*[22]

Spike sorting and selection of responsive neurons in microwires

Three patients had microwires (Behnke-Fried electrodes,[21] Ad-Tech Medical) in the insula protruding from the electrode tip (Fig. 1b '+'). Spikes were detected and sorted using Wave_Clus2.[23] In short, raw data was filtered between 300-3000 Hz. As per default settings, spike waveforms were extracted from 0.625 ms before to 1.375 ms after the signal exceeded a 5*noise threshold, where noise was the unbiased estimate of the median absolute deviation. The waveforms were sorted and clustered by Wave_Clus2 automatically and were then

manually checked by author RB. Clusters were excluded if more than 2% of spikes were observed within an inter-spike interval of 2 ms or if firing rate was less than 1 Hz. To identify cells that responded to our stimuli, we used a Wilcoxon signed rank test comparing spike counts during baseline (-1 s to 0 s) against that during the pain period (1 to 2 s) for Hand and Face trials together. Only cells that showed a response to the stimuli (p_t<0.05), irrespective of pain intensity, were considered for further analysis.

Intensity coding in spiking activity

Similar to LFP analyses, a cell was said to show *intensity coding*, if spike counts correlated positively with reported intensity. Because JASP includes Bayesian statistics using Kendall's Tau, but not Spearman's r, we used the former to quantify evidence for or against intensity coding.

Broadband power analyses in microwires

To explore whether intensity coding in cells and the broadband power (BBP, 20-190 Hz, Fig. 2b) from the same microwire were related, for the 10 microwires that yielded responsive neurons (whether these neurons showed intensity coding or not) we quantified the association between BBP averaged over the pain period (1-2 s) and intensity ratings (1-2, 3-4, 5-6, 7-8) using rank correlation coefficients separately for face and hand videos (again using Kendall's Tau to provide BF_{+0} estimates). All 8 microwires protruding from the same electrode were first re-referenced to the microwire with the least spiking and lowest artefacts, yielding seven microwire recordings for each of the 4 electrode tips with wires in the insula. Data were filtered to remove 50 Hz noise and harmonics at 100 and 150 Hz. Subsequently, they were separated into trials of 4 s (-1 s to 3 s relative to video onset), down-sampled to 400 Hz, and visually checked for artifacts. The time-frequency decomposition of power followed the same procedure as for the macro-contact recordings. Finally, intensity coding at the level of spikes (r_K(spikes,rating)) and BBP (r_K(BBP,rating)) from the same wire were compared using a Kendall's Tau coefficient.

fMRI experiment

Twenty-five healthy volunteers performed a task similar to that used in the iEEG recordings while brain activity was measured using fMRI at 3T as detailed in Supplementary Note 10.

Data availability

The data presented in this work are available upon request.

Results

Comparing the ratings of the seven patients that were included in our final analysis with those of an age- and gender-matched control group revealed that the ratings of the patients were in the normal range (Supplementary Note 1).

iEEG activity in the insula correlates with the perceived intensity of the pain of others

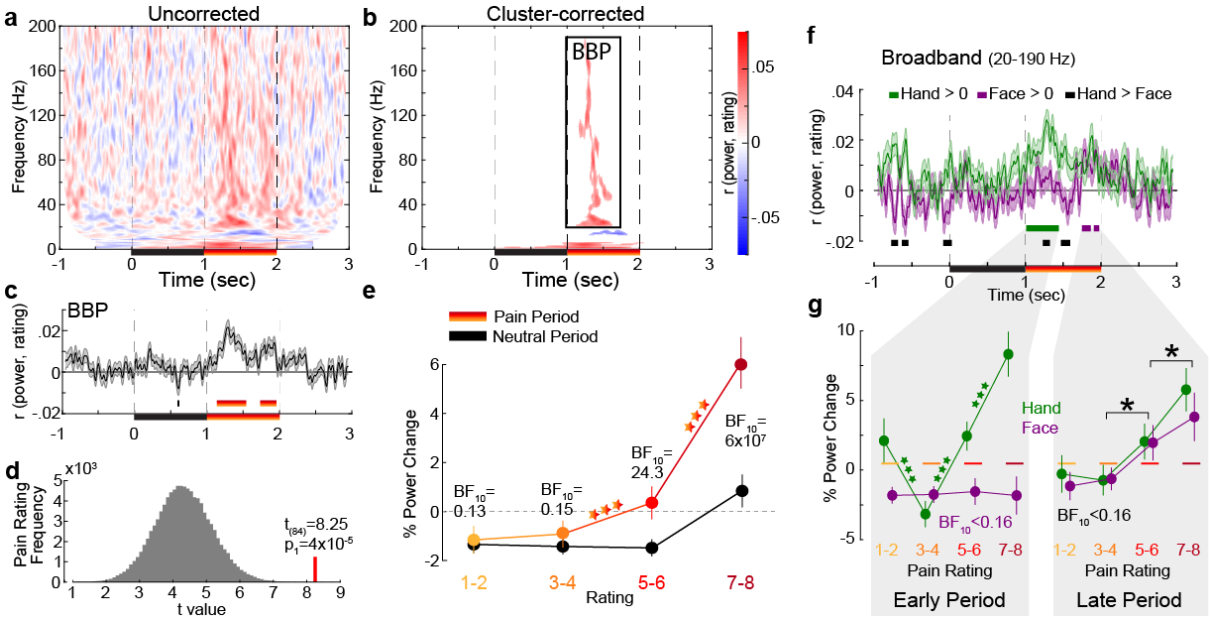

Figure 2 Intensity coding in the local field potentials from macro-contacts in the insula. (a) For each frequency and time relative to stimulus onset, the average r_S-value over all insular bipolar recordings between iEEG power and rating for Face and Hand trials together. **(b)** The same as (a), but cluster corrected for multiple comparison as described in Supplementary Note 5.1.[45] BBP: Broad-Band Power, the cluster of significant positive intensity coding frequencies (i.e. r_S>0, 20-190 Hz) used throughout the paper. **(c)** Mean±sem time course of intensity coding in BBP over the 85 recordings when Face and Hand trials are combined. Above the x-axis, orange bars show periods of significant intensity coding after circular shift correction as defined in Supplementary Note 5.1 during the pain period, the brief black bar indicates negative correlation significance during the neutral period. Below the x-axis, the black block marks the neutral and the warm block the pain period. **(d)** The t-value of a t-test comparing the intensity coding of all 85 bipolar recordings combining Hand and Face trials within the pain period (1–2 s post-stimulus onset) in the insula against zero (red) was higher than the distribution of corresponding t-values obtained when performing the same test using 85 bipolar recordings randomly selected 100,000 times from the macro-contacts of our 7 patients anywhere in the brain (Supplementary Note 5.4). **(e)** Mean±sem % BBP changes relative to baseline as a function of reported intensity separately for the neutral (black) and pain (yellow-red) period when combining Hand and Face trials. BF_{10} values: Bayes-factor quantifying evidence for H_1 relative to H_0 from a non-parametric t-test comparing BBP power during the pain period against that during the neutral period. ***: p<0.001 relative to the preceding reported intensity. See Supplementary Note 5.3 for ANOVA details. **(f)** Time course of intensity coding in BBP for Hands and Faces separately. r_S>0 indicated with green bars for Hands and purple for Faces. Black bars indicate r_{S_Hand}>r_{S_Face}. The early and late periods that result for Hands and Faces, respectively, will be used throughout the paper. **(g)** Mean±sem BBP as a function of rating for Hands and Faces in the early and late periods. Green ***: p<0.001 relative to the preceding intensity for the Hand. Black *: p<0.001 main effect of rating (i.e. combining Hand and Face) similar to panel (e). Purple BF_{10}: evidence for a lack of difference across ratings for the Hand. Black BF_{10}: lack of difference between rating 1-2 and 3-4 with Hand and Face combined.

Plotting the power over the bipolar electrodes as a function of perceived intensity, irrespectively of whether Hand or Face movies were shown (Supplementary Fig. 3a-d) suggests an increase in power for the highest ratings. Correlating power with reported intensity and applying cluster corrections (Supplementary Note 5.1) revealed a cluster of positive correlations ranging from 20-190 Hz and 1.12-1.62 s (p_1<0.001; p_1=one-tailed p value); one at very low frequencies (1-6 Hz, 0.02-2.055 s; p_1<0.001), and a small cluster of negative correlations (13-17 Hz, 1.295-1.83 s; p_1=0.004; not further discussed, Fig. 2a-b). Intensity coding was apparent in all traditional frequency ranges, except alpha

(Supplementary Note 5 and Supplementary Fig. 3f-g) and, as expected, was significant during the pain period. With no obvious differences among frequency bands above alpha, we henceforth used the frequency band 20-190 Hz for all analyses and refer to it as broadband power (BBP). We concentrate on BBP rather than oscillatory signals in lower frequencies because BBP is more closely linked to neural spiking,[24–26] and cannot be explored in non-invasive EEG recordings. The temporal profile of the BBP-rating association revealed two periods with significant positive correlations: 1.1375–1.54 s and 1.7375–1.9575 s (Fig. 2c). Averaging BBP power over the entire pain period revealed that, out of 85 macro contacts, 27 (32%) showed a significant positive correlation (assessed as p_1<0.05, Supplementary Fig. 3k) between perceived intensity and BBP (all r_S[118]>0.156, p_1<0.045), which was extremely unlikely to occur by chance (Binomial p_1=5x10^{-15}, BF_{+0}=3x10^{12}). Also, randomly picking 85 electrodes anywhere in the brain yielded BBP-rating associations that were significantly lower than those we find in the insula (p_1=4x10^{-5}, Fig. 2d and Supplementary Note 5.4), confirming that the BBP in the insula has enriched intensity coding. The effect of reported intensity depends mainly on BBP power increases for the two highest intensity ratings (Fig. 2e and Supplementary Fig. 3a-e).

Intensity coding arises earlier for the Hand than Face stimuli

To investigate how intensity coding depends on the stimulus, we then separated Face and Hand trials. The time-frequency analysis revealed regions of broadband intensity coding earlier for Hand than Face, as reflected in a direct comparison (Fig. 2g, and Supplementary Note 5.5). Focusing on the BBP frequency range identified independently of stimulus type, significant intensity coding for the Hand from 1.0075 to 1.4375 s (hereafter 'early period') and for the Face from 1.75 to 1.8625 s and from 1.905 to 1.975 s, which jointly (1.75-1.975 s) will be called 'late period' (Fig. 2h). The insula thus reflects in broadband activity the perceived intensity with differential time courses for hand and face videos in the current study.

To explore the shape of the BBP-rating relation, we averaged BBP over time for the early and the late periods for each pain rating separately (Fig. 2i). For the early period, a stimulus (Hand, Face) x rating repeated-measures ANOVA revealed a significant interaction (Greenhouse-Geisser-corrected F[2.183,102.621]=13.55, p=3x10^{-6}, BF_{incl}=2x10^6). Planned comparisons provided evidence that BBP for Faces in the early period was similar for consecutively increasing painfulness level pairs (all t[47]<0.252, p_2>0.802, BF_{10}<0.163), whereas, there was an orderly increase in broadband power for increasing pain ratings for Hands from 3-4 onwards (3-4 vs 5-6: t[47]= 5.97, p_2=3x10^{-7}, BF_{10}= 51110; 5-6 vs 7-8: W= 188, p_2=2x10^{-5}, BF_{10}= 764.63). However, BBP for ratings of 1-2 was unexpectedly higher compared to the ratings of 3-4 (W=1014, p_2=3x10^{-6}, BF_{10}= 847.14). A similar ANOVA for the late period, revealed evidence for the absence of an interaction (F[3,141]=0.55, p_2=0.650, BF_{incl}=0.034). There was only a significant main effect of rating (F[3,141]=16.54, p=3x10^{-9}, BF_{incl}=2x10^7), indicating that BBP in the late period of the Hand and Face videos together was the same for ratings 1-2 and 3-4 (W= 597, p_2=0.931, BF_{10}= 0.163), but thereafter showed significant increases with each consecutive increase in pain ratings (3-4 vs 5-6: t[47]= 3.46, p_2=0.001, BF_{10}= 25.147; 5-6 vs 7-8: t[47]= 2.90, p_2= 0.006, BF_{10}= 6.292). Taken together, these analyses indicate BBP in the insula reflects perceived intensity only for the Hand stimuli in the early, and for both stimulus types in the late window.

Motion information relates to Hand responses and Shape information to Face responses

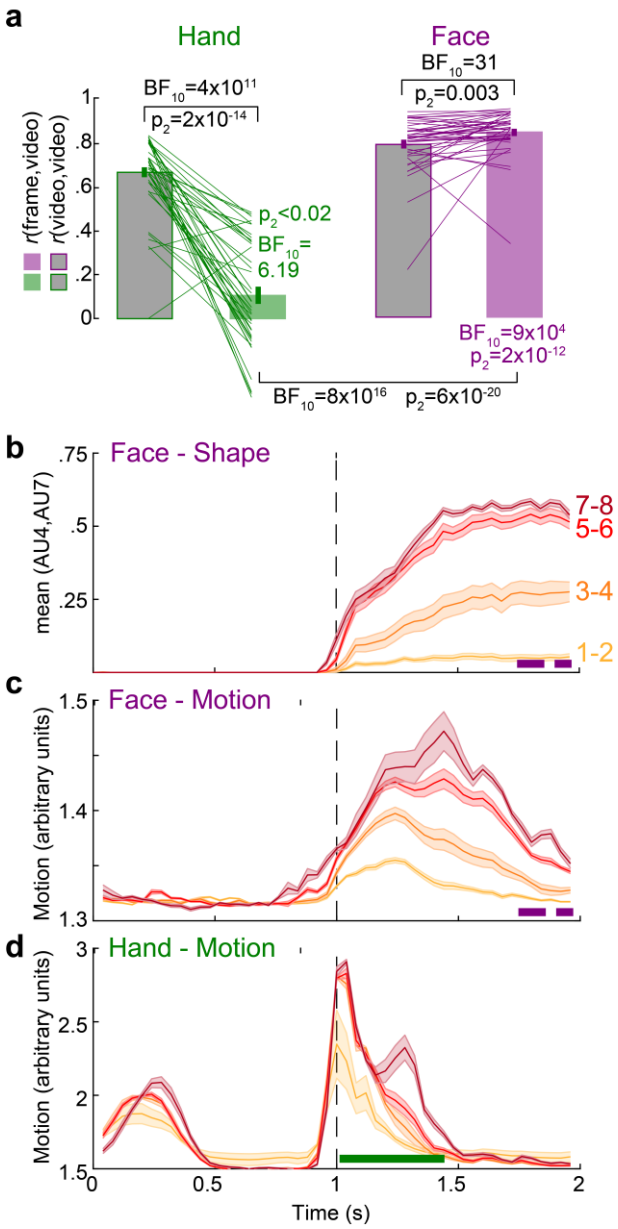

Figure 3 Temporal dynamics of pain perception. **(a)** Mean±sem of Spearman correlation between each participant in the frame rating task and the average ratings of the other participants in the video rating task (r_S(frame,average_video), green and purple) compared against that between the participants rating of the video and the average rating of the other participants in the video rating task (r(video,average_video), gray) for Hands and Faces. Black statistics above the bars compare the respective frame and video rating, the colored statistics compare the frame rating against zero. The black statistic under the bars compare the frame rating across Hand and Face. See Supplementary Notes 6.1 for additional methods and analyses. **(b)** The average activation of the Action Units (AU) 4 and 7 was used to estimate the intensity of the shape information in Faces. Mean±sem shape estimation as a function of time for Face videos rated as 1-2, 3-4, 5-6, 7-8. Purple bars indicate the period with significant BBP-rating correlations for Faces, as seen in Fig. 2f. **(c)** The same as (b), but for motion information in Face videos. **(d)** The same as (c), but for motion information in Hand videos. Green bar shows the period with significant BBP-rating correlations for Hands, as in Fig. 2f.

To shed light onto the contribution of kinematic and shape information in the stimuli to the intensity coding in the insula and the differences in response timing for Hand and Face videos, we subjected our stimuli to more detailed, time-resolved analyses (Supplementary Note 6). Regarding shape information, psychophysics on a subset of 40 participants from our original online video rating revealed that they can recognize the pain intensity of Face stimuli from static frames taken at key moments in the stimuli with accuracy even better than that for the entire video (W=193, p_2=0.003, BF_{10}=31.293, Fig. 3a). The accuracy for the Hand instead dropped significantly (t[38]=11.959, p_2=2x10^{-14}, BF_{10}=4x10^{11}). This suggests that static shape information could suffice to explain ratings for Face, but not Hand stimuli. Using the automated face analysis software FaceReader to extract the two most reliable shape features of painful facial expressions (facial Action Units AU4 and AU7)[27], we find that how lowered the eye brows (AU4) and how tightened the eye lids are (AU7) in key frames suffices to predict participants' perceptions of the pain intensity in Face stimuli with r_p=0.95 accuracy

(Supplementary Note 6.2), and we thus use the average time-course of these two AUs to track shape information in our Face stimuli (Supplementary Fig. 5a). Figure 3b shows shape information increases towards the end of the movies with rating intensity. Comparing the timing of intensity coding for the Face in the insula BBP (purple bar in Fig. 2f and 3b) with the timing of the shape information for the Face (separation between the curves in Fig. 3b) shows a nice correspondence, with both highest late in the movie. Regarding kinematics, we calculated the changes in pixel values across consecutive frames to track the timing of motion (Fig. 3c,d), and this information could also predict the rating of our patients with high accuracy for both stimulus types (Supplementary Fig. 5c). Comparing the timing of intensity coding in the insula with that of motion information provides contrasting results for the Face and Hand stimuli. While for the Hand, neural intensity coding (green bar in Fig. 3d) and motion information are both strong early in the pain epoch, for the Face, neural intensity coding (Fig. 3c purple bar) maximizes when motion information has already declined. This suggests that shape information could dominate Face intensity coding, while motion information could dominate Hand intensity coding. A more quantitative approach that estimates how much motion and shape information predict our patients' ratings on a frame-by-frame basis and how the neural intensity coding lags behind this information (Supplementary Note 6 and Supplementary Fig. 5g) confirms this analysis, and provides some estimates of the latency with which the insula responds to these sources of information: for Face stimuli, the insula response lags behind the shape information by 40-320 ms, while for the Hand stimuli, the insula response lags behind the motion information by 0-80 ms.

The insula contains a surprising number of stimulus-specific intensity coding locations

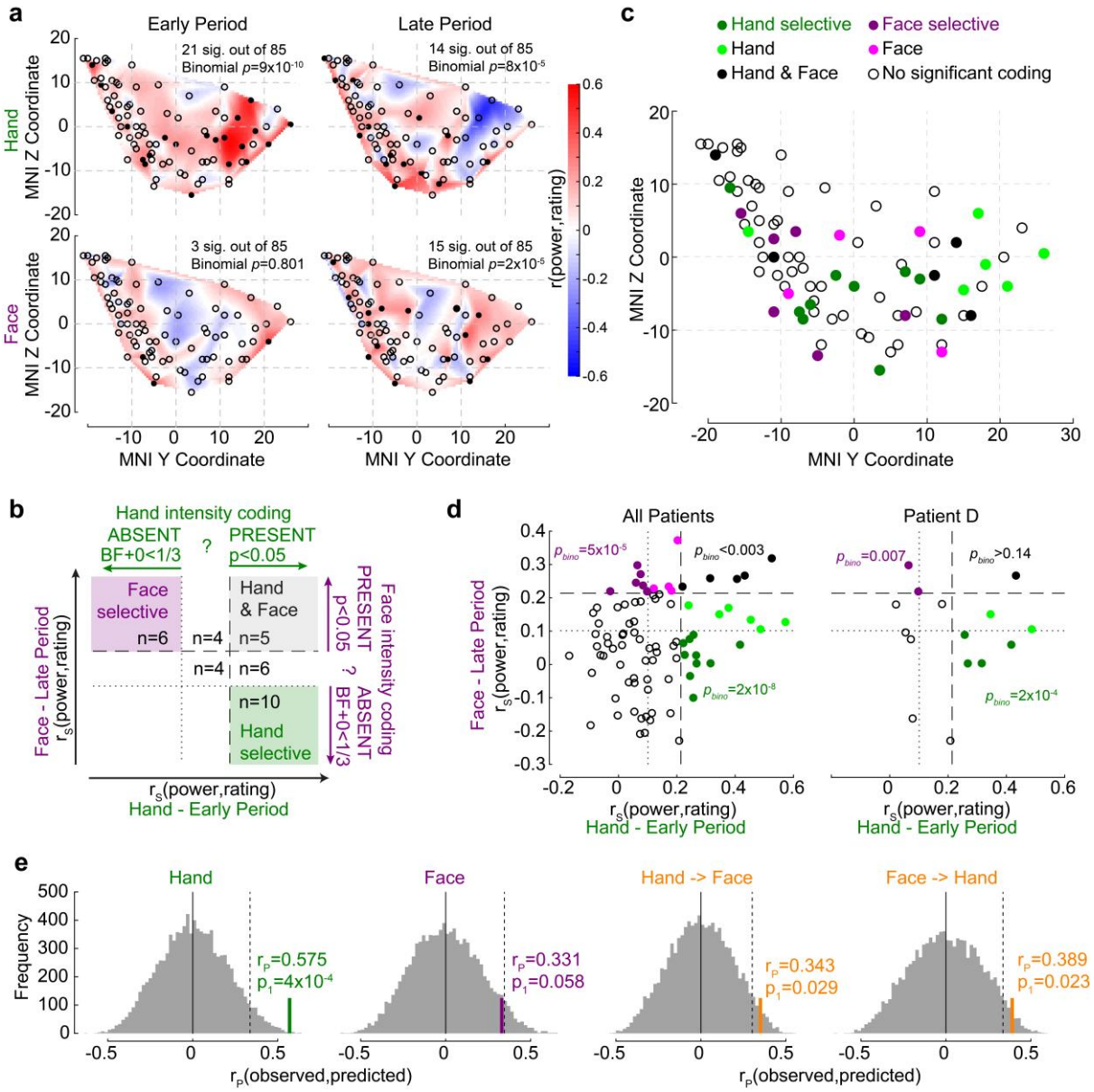

Figure 4. Relation between hand and face intensity coding in the insula. (a) Topographical maps of BBP-rating correlation coefficients for Hands and Faces in the early and late periods. Each circle is one of the recording sites (as in Fig. 1b), with filled circles indicating locations with significant correlation coefficients (p_1<0.05). **(b)** Classification of recording locations based on their Hand (early period) and Face (late period) intensity coding. Bipolar recordings in the gray zone (n=5) significantly co-represent intensity for Hands and Faces (both p_1<0.05, i.e. beyond dashed line). Recordings in the purple (n=6) and in the green (n=10) zone represent intensity coding selective for Faces or Hands, respectively, i.e. one p_1<0.05 and one BF_{+0}<⅓. **(c)** Location of all 85 bipolar recordings color-coded by selectivity as described in (b). Note that locations Hand and Face without further specification are those with r_S values for the other stimulus type falling between the dashed and dotted line, that provides inconclusive evidence, and thus show neither significant dual coding, nor evidence of absence. Open circles represent all locations with p_1>0.05 for both Hand and Face. **(d)** Correlation coefficients for Hands and Faces separated by coding characteristics in (b) for all patients together and for an exemplary patient. p_{bino} refers to the likelihood to find the observed number of locations in that quadrant using a binomial distribution as explained in Supplementary Note 7. **(e)** The left two panels depict the average pearson correlation coefficients, together with corresponding resampling null distributions, as a measure of the accuracy of decoding intensity ratings using the partial least square regression (PLSR) beta coefficients of BBP in the early period for Hands and in the late period for Faces as described in Supplementary Note 8. The right panels

are similar to left panels, but show the accuracies of cross-decoding, predicting Hand ratings from the Face BBP and vice versa. The dotted lines indicate 95th percentiles of the resampling null distributions.

We next focused on how individual recording sites reflected perceived intensity. In the early period, for Hand videos, 21/85 (25%) showed significant intensity coding (rating-BBP correlations, all $r_S[58]>0.219$, $p_1<0.046$), which was above chance (Binomial, 21/85 at $\alpha=0.05$, $p_1=9x10^{-10}$, $BF_{+0}=2x10^7$). In contrast, for the Face, only 3/85 showed intensity coding (4%), which is expected by chance (Binomial $p_1=0.804$, $BF_{+0}=0.025$). During the late period, above chance numbers of recordings showed intensity coding for Hand (14/85, 17%, $p_1=8x10^{-5}$, $BF_{+0}=201.41$), and the same was true for Face videos (15/85, 18%, Binomial $p_1=2x10^{-5}$, $BF_{+0}=808.49$; Fig. 4a).

If the insula simply represents salience, one might expect a tight association between intensity coding for the Hand and Face, and an above chance number of locations showing intensity coding for Face and Hand. In contrast, if the insula also represents more specific information, we would expect above-chance numbers of locations with intensity coding for the Face, but not the Hand and vice versa. Statistically, we inferred the *presence* of intensity coding based on $r_S>0$, $p_1<0.05$, like elsewhere in the manuscript, and its *absence* using Bayesian statistics,[22] with $BF_{+0}<⅓$. Plotting each bipolar recording's r_S values on an x-y plot, with x representing r_S for the Hand and y for the Face, with dashed and dotted lines at critical r_S values corresponding to $p_1<0.05$ and $BF_{+0}<⅓$, we defined 9 quadrants, three of which are of conceptual importance (Fig. 4b): those of locations with dual intensity coding (i.e. $p_1<0.05$ for Face and Hand), those with Face-selective intensity coding (i.e. Face $p_1<0.05$, but Hand $BF_{+0}<⅓$) and those for Hand-selective intensity coding (i.e. Hand $p_1<0.05$ but Face $BF_{+0}<⅓$). We then used binomial tests to compare the proportion of locations falling in these three quadrants against chance, and found that all three quadrants contain more locations than expected by chance (Fig. 4d and Supplementary Note 7 for details of the statistics and why for $BF_{+0}<⅓$, false negative $p\approx0.05$)[22,28]. Indeed, even within a single patient, amongst simultaneously recorded channels, we find above chance numbers of Face and Hand-selective channels (Fig. 4d). Also, calculating the association between intensity coding across Hand and Face through a simple correlation of the respective r values confirms the presence of a significant but weak and barely worth mentioning (in a Bayesian sense) association ($r_K=0.131$, $p_1=0.038$, $BF_{+0}=1.27$). Together, this shows the insula is a patchwork, with some locations representing the Hand but not the Face, others the Face but not the Hand, and a small number finally representing both in terms of intensity coding. The spatial distribution of these locations is shown in Fig. 4c.

In addition, we used a multivariate partial least square regression (PLSR) approach to assess how well the pattern of BBP across the insula can predict participants' pain ratings (Supplementary Note 8). BBP across the 85 sites in the early period for Hand videos can be used to predict the patients' average rating of the stimulus with reasonably high accuracy ($r_P=0.575$, $p_1=9x10^{-4}$), and BBP in the late period for Face videos with almost significant accuracy ($r_P=0.331$, $p_1=0.058$, Fig. 5e). To test if intensity was encoded similarly for the two stimulus types, we repeated the analyses training the PLSR on one stimulus type and testing it on the other. We found above-chance cross-decoding in both cases (Fig. 4e). However, when the 5 contacts that significantly co-represented pain intensity for both hand and face videos (the black dots in Figure 4c) were excluded from the analyses, the cross-decoding accuracy fell to insignificant levels (Hand->Face: $r_P=0.175$, $p_1=0.153$; Face->Hand: $r_P=0.185$, $p_1=0.149$). These findings corroborate the above results, indicating that perceived pain intensity is reflected in the insula as a mixture of hand-specific, face-specific, and hand-face common representations.

Hand intensity coding increases anteriorly as in a similar fMRI task

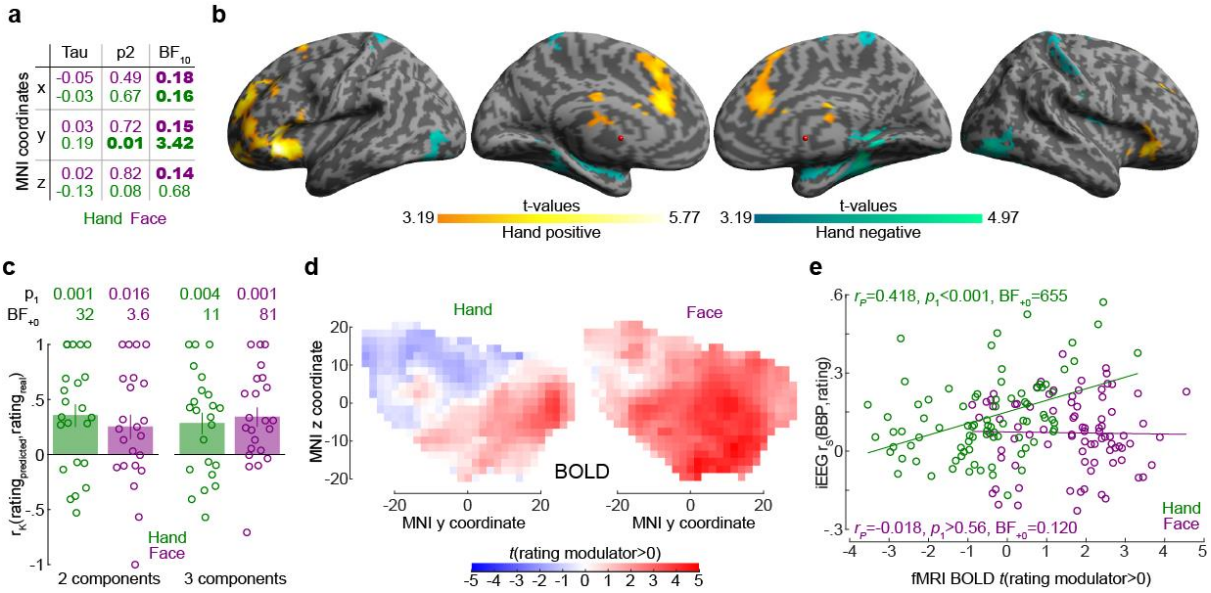

Figure 5. **Relationship between BBP and BOLD activity and intensity coding. (a)** Correlation (r_K) between MNI coordinates and BBP intensity coding, separately for Hand (green) and Face (purple). Bold numbers mark evidence for (BF_{10}>3) or against (BF_{10}<⅓) a correlation. Statistical values were obtained by correlating separately the x, y or z coordinate of each bipolar recording with the r_S(BBP,rating) of each recording over all 85 recordings using JASP. Tau refers to Kendall's Tau, *p2* and BF_{10} the two-tailed probability and BF based on H_0:Tau=0. **(b)** Results of the regression analysis between resting state connectivity and intensity coding for the 85 bipolar recording coordinates for the Hand. Warm colors indicate significant positive, and cold, negative regression values. **(c)** Predictive performance of a PLSR trained to predict ratings based on the pattern of BOLD activity across all voxels in the insula for different ratings. A leave-one-out cross-validation was used, and each circle represents the r_K between the predicted and actual rating for each left out participant, and the p_1 and BF_{+0} values then test these n=23 correlation values against zero using a non-parametric association test (Kendall's Tau). Results are shown as mean±sem separately for Hand and Face trials, and using 2 or 3 components. See Supplementary Note 10.5 for details. **(d)** Topography of intensity coding for the Hand (left) and Face (right), as assessed at the group level, by the parametric modulator capturing changes in BOLD activity that correlate with trial-by-trial differences in participant's rating. t-values testing the parametric modulator >0 at the group level are shown as a function of y and z coordinate in the insula mask. For each coordinate, the maximum value across all x-coordinates within the two insulae is indicated. **(e)** Relation (r_P because of normality) between the t-value of the parametric modulator for the rating in the fMRI bold data (x-axis) and the BBP intensity coding (computed in the early period for the Hand, green, and late period for the Face, purple) in the iEEG signal (y-axis) for each of the 85 contact locations. Note that for the fMRI signal, the value is taken from the voxel closest to the MNI coordinates of the corresponding contact in the iEEG signal.

To examine the spatial distribution of intensity coding, we examined the relationship between MNI coordinates of the bipolar recordings and intensity coding (i.e. r_S(BBP,rating), Fig. 5a). The only significant association was that more anterior recordings (i.e. more positive y-coordinates) have higher Hand intensity coding. Interestingly, we found evidence against a right-left difference (i.e. BF_{10}<⅓ for x-coordinates) for the Face and Hand, providing moderate evidence against a left-right lateralization.

To better understand the origin of the anterior gradient for Hand intensity coding, we performed a regression analysis between intensity coding of the 85 insular recording locations (for Hand and Face separately), and resting state connectivity seeded at corresponding MNI locations in Neurosynth (see Supplementary Note 9). Insular locations with higher Hand intensity coding had higher resting state connectivity with the left anterior

insula and ventral prefrontal cortex (including BA44/45, OP8/9, Fp1), with the right frontal orbital cortex; with the bilateral cingulate (incl. BA24/33); and the right cerebellum (Crus I and lobules VI, VII and VIII) ($pFWE_C$<0.001, t=3.19; Supplementary Table 3). In line with the lack of spatial gradients for the Face stimuli in the insula of our patients, examining which voxels had higher resting state connectivity with insular locations with higher Face intensity coding did not yield significant results (p_{unc}>0.001, t=3.19).

Finally, to compare the spatial gradient we find using iEEG with that using fMRI, we leveraged existing data from an unpublished study in our lab using a similar design to measure brain activity using fMRI in healthy participants (Supplementary Note 10). BOLD activity in the insula also contained significant information about the perceived intensity for Hand and Face stimuli (Fig. 5c). For both the Hand and the Face stimuli, we found a gradient along the y axis with more anterior locations showing a stronger, and more positive association between BOLD activity and rating (Fig. 5d). For the Hand, across our 85 bipolar recordings in the patients, locations with higher BBP intensity coding in iEEG also show higher t-values in the BOLD signal (Fig. 5e). For the Face, we have evidence of absence for an association of the two measures (Fig. 5e).

The insula contains neurons with intensity coding for the Hand and/or Face

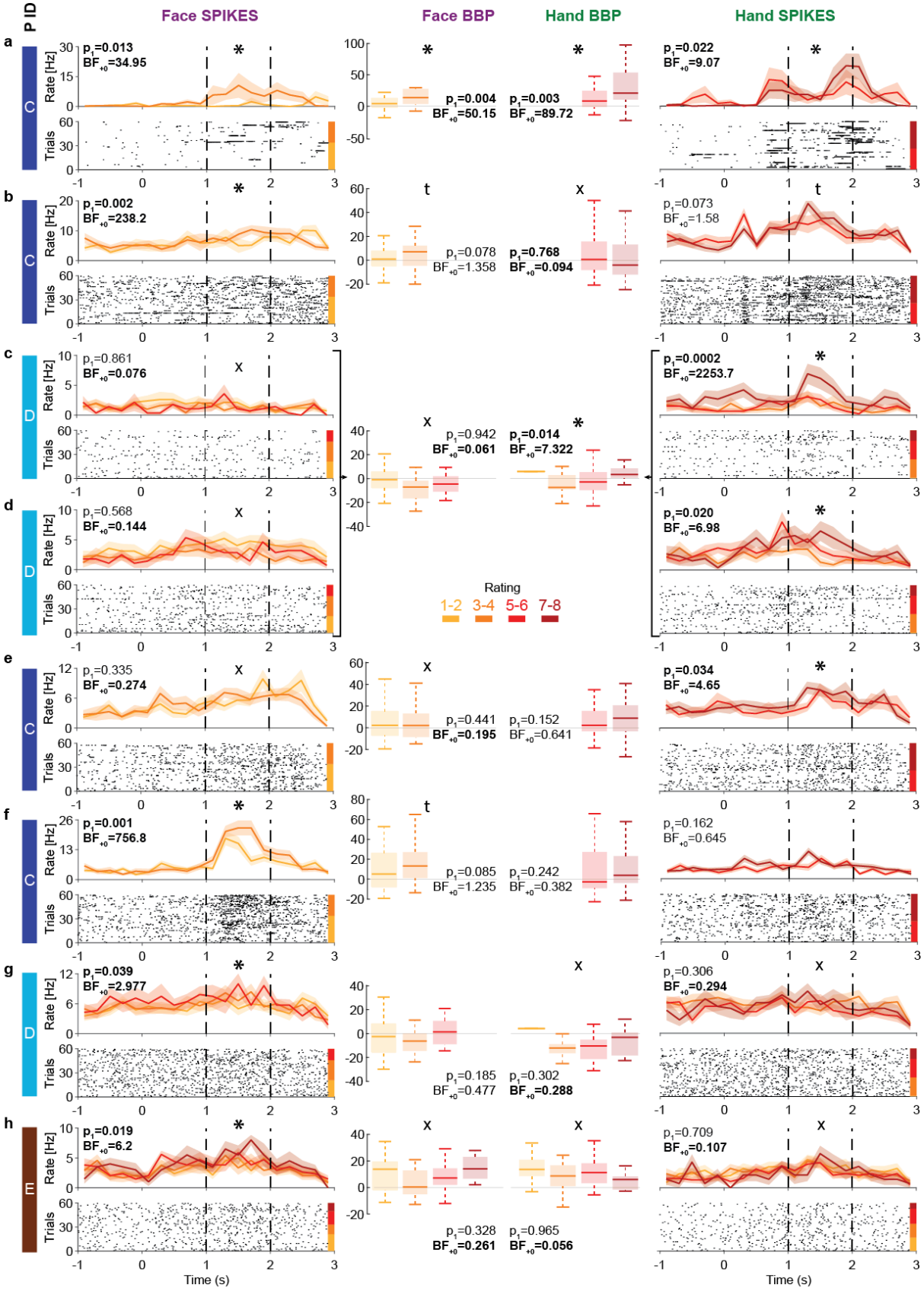

Figure 6. Intensity coding in single cells and corresponding local field potentials. (a-h) Left (Face) and right (Hand) columns display, for each cell, the rastergrams and peri-stimulus time histogram (PSTH) for 8 cells that showed intensity coding for at least one stimulus type. For the PSTH, each curve represents the mean±sem of the firing rate in each bin for trials with the corresponding rating. Not all patients gave all possible ratings in each condition. For the rastergram, trials are sorted in order of rating, with the highest ratings upmost. The colorbar next to the rastergram indicates the rows corresponding to each rating. p_1 and BF_{+0} values result from a one-tailed test of the Kandell's Tau between rating and spike-count in the pain period (marked by the dashed lines). *= significant intensity coding (p_1<0.05), t= trend (p_1<0.1), X= evidence of absence for a positive intensity coding (BF_{+0}<⅓). The x-axis (time) is relative to movie onset. The color bar on the leftmost side indicates from which patient the data is taken. Middle columns show the BBP averaged over the pain period for the corresponding microwire as a function of rating as a boxplot showing the variance across trials, with the box and whiskers representing the quartiles across trials, and the p_1 and BF_{+0}, the Kendall's Tau test of the association of rating and BBP. Note that cells c and d were taken from the same microwire, and therefore have only one BBP graph.

The insula thus displays intensity coding in a broad frequency range, including locations with Hand- or Face-specific intensity coding, as well as locations showing intensity coding for both stimulus types. To explore this representation at the level of single neurons, we analyzed the microwire data from the 3 patients (patients C, D, and E) that had microwires in the ventral anterior insula (see '+' symbols in Fig. 1b for locations and Supplementary Table 2). Spike sorting resulted in a total of 28 candidate neurons. From these, 13 showed more spikes during the pain period than the pre-stimulus baseline. Amongst those, 8 show intensity coding for the Face and/or Hand (Fig. 6), with significant Kendall's Tau correlations between perceived intensity (1-2, 3-4, 5-6, 7-8) and spike count during the pain period (1–2 s post-stimulus onset) for at least one stimulus type: 4/8 for the Face and 5/8 for Hand (Binomial, Face: p_1= 0.003, BF_{+0}=27; Hands p_1=3x10^{-4}, BF_{+0}=282). Considering the p_1-value for the intensity coding, two cells (a,b) showed intensity coding for both hand and face trials, 3 (c-e) only for hand and 3 (f-h) only for face trials. If we additionally consider the BF_{+0} values below ⅓ as evidence for the absence of coding in the other stimulus type, we find 3 Hand-specific cells (c,d,e) and 2 Face-specific cells (g,h). Importantly, within patient D, we observe the co-existence of Hand-selective (c,d) and Face-selective intensity coding (g).

To explore how spiking relates to BBP, we analysed the BBP from the 10 wires that yielded the 13 cells showing stimulus triggered responses. Using Kendall's Tau correlations between BBP (20-190 Hz) and the patient's intensity ratings (1-2, 3-4, 5-6, 7-8), and comparing these results with the coding of the cells on the same wire reveals some relationship between the two. For the Hand videos, two out of three wires that yielded cells with intensity coding also showed significant association of ratings and BBP (Fig. 6a,c,d). Indeed, intensity coding (i.e. correlation between intensity rating and spiking/BBP) were significantly correlated across the 10 microwires (r_K=0.57, p_1=0.012, BF_{+0}=7.69). For the Face videos, only 1/5 wires with spike intensity coding cells showed significant intensity coding in the BBP, and 2/5 showed a trend. Across the wires, there was a trend towards an association between the intensity coding in the spikes and BBP (r_K=0.34, p_1=0.088, BF_{+0}=1.63).

Discussion

To our knowledge, the present study provides the first detailed profile of how intracranial LFP and some single-units in the human insula reflect the perceived intensity of pain experienced by others. LFPs indicate that neural activity in the insula within a broad range of frequencies, including the conventional theta, beta and gamma frequency bands, scales with the perceived intensity of pain expressed by others. Interestingly, the insula only appeared to be recruited once the perceived pain level was at least moderate: activity was increased for

moderate (5-6) compared to mild (3-4) and for severe (7-8) compared to moderate. However, activity for mild pain (3-4) was not significantly increased compared to minimal pain (1-2), or baseline activity. This echoes a recent finding that BBP activity in the insula is selectively increased when heat-stimulation becomes truly painful.[12] Furthermore, we isolate a small number of insular neurons increasing their firing with increases in the intensity of pain experienced by others.

The human insula has historically been in the focus of pain neuroscience as part of the pain matrix recruited by first-hand experience of pain.[29] In this tradition, neuroimaging evidence for activation of the insula while witnessing pain experienced by others has lead many to suggest it may represent a neural basis for empathy for pain.[1,3,4,30] In contrast, the insula has been more recently conceptualized to represent any stimuli that are behaviorally critical for the organism in a given situation, challenging the historical notion that it selectively represents pain.[31–33] In the present study, we do not intend to (and cannot) address the selectivity of the insula for pain over other salient stimuli, and we do not claim the neural responses we report are pain-specific. Instead we characterize how the insula's iEEG activity encodes the intensity of other people's emotions, using pain as an important category, and use the agnostic terminology of 'intensity coding', rather than 'pain intensity coding' throughout the paper.

An important, and somewhat related, question has been whether pain or salience cues are represented in a modality-specific or modality-general manner in the insula. fMRI studies have shown that the anterior insula is coactivated with different brain regions depending on whether the pain of others is conveyed via indirect cues or via the actual body part, such as the hand, that directly receives the noxious stimulation.[1–4,17] Here, we provide electrophysiological measures of neural activity that speak to that issue. We focus on the broad-band gamma signal known to have comparatively high spatial specificity and be closest to neural spiking,[24–26] and find a mixed organization, consisting of modality-specific and -general locations in a partially intermixed layout: we found locations with broadband activity and spiking associated with perceived intensity for the Hand, but not the Face; others associated with the Face, but not the Hand; and others still associated with perceived intensity for both.

Leveraging our high temporal and spatial resolution, we found that locations that showed intensity-coding for the Hand stimuli have activity timing echoing the timing of motion cues with relatively short latencies <100 ms. Locations that show intensity coding for the Face appear to have activity echoing the timing of shape information with latencies no longer than 320 ms. These latencies are in a range similar to that found following nociceptive stimulation[12] or static disgusted facial expressions.[34,35] Using automated software to detect the level of activation of the facial action units 4 and 7 (i.e. lowering eye-brows and tightening eye-lids), we find that this information suffices to predict participants' rating of the stimuli with high accuracy, and followed the time course of the neural activity in the Face intensity encoding locations well enough to suggest that it provides traction on the analyses of dynamic pain-related facial expressions.

An important consideration is whether this selectivity for Face or Hand stimuli could simply originate from some participants finding our facial stimuli more salient, and others the hand stimuli. That we find face and hand selectivity side-by-side in simultaneously recorded locations and neurons in single patients suggests that this cannot suffice to explain our data. On the other hand, we also found evidence that some locations and cells represent intensity coding for both the Hand and the Face stimuli, and overall, if we train a partial least square regression to predict perceived intensity from the activity pattern across all recorded

locations, we find that training the decoder on Hand activity pattern and testing it on Face activity patterns (or vice versa) leads to above chance decoding. This confirms that the insular representation of intensity can support stimulus independent decoding - despite our partial least square regression not being biased to focus on signals that do generalize well across stimulus types. This provides an electrophysiological basis for recent fMRI studies that show that stimuli depicting situations in which others' experience of pain or not can be discriminated using the same pattern across hand and face stimuli.[36]

In addition to the broadband results we report in detail, we find that theta power increases with perceived intensity. Given a growing animal literature establishing that interareal theta synchronization promotes learning about threats,[37–39] examining the coherence in the theta range across iEEG electrodes in different brain regions during pain observation may in the future shed light on how humans learn about safety through others.

Spatially, finally, we found that Hand intensity coding was enriched in the anterior dorsal insula, where we also found the largest proportion of locations encoding both Hand and Face intensity. This anterior bias was also observed in our BOLD signal for similar Hand stimuli. A recent meta-analysis identified that the most consistent BOLD activations when observing limbs in painful situations within the insula occur bilaterally around MNI coordinates y=13 and z=10,[4] which closely matches where we find the highest density of Hand intensity coding (Fig. 5a). Interestingly, locations with higher Hand intensity coding have increased connectivity at rest with extra-insular regions involved in processing two relevant stimulus dimensions. Connectivity was higher with cerebellar lobules VI, VII, and VIII, and with the inferior frontal gyrus, all of which are recruited by[40–42] and necessary for[42–44] perceiving the very kinematics of hand actions we find to be good predictors of BBP activity in the current study. Connectivity is also higher with the mid- and anterior cingulate cortex associated with pain witnessing in humans[1,3,4] and that contain neurons with pain intensity coding in rats witnessing the pain of other rats.[7] Somewhat surprisingly, we did not find a clear spatial clustering of Face intensity coding in our electrophysiological data. This contrasts with our BOLD data, where face intensity coding was stronger more anteriorly, and with meta-analyses that show the left anterior insula to be reliably recruited by the observation of painful facial expressions.[4] However, that we find fewer locations and less reliable spatial organization for Face than Hand intensity coding could help explain why both recent meta-analyses of the fMRI literature show that, when comparing studies showing limbs in painful situations with those showing painful facial expressions, the insula is more reliably recruited by the sight of limbs.[3,4] Indeed, that we find a macroscopic organization for the Hand, but not the Face, intensity coding is echoed at the mesoscale: microwires with cells with Hand intensity coding also tend to show Hand intensity coding in the BBP signal that is thought to pool the spiking of many neighbouring neurons, but the same is not true for the Face. In terms of lateralization, we find that our data is more likely if one assumes that both hemispheres have similar intensity coding, than if one hemisphere were dominant. This echoes the fact that during noxious stimulation on the right hand, both insulae show significant iEEG responses (although slightly stronger in the left insula)[12] and that fMRI fails to find robust lateralization of responses to empathy for pain.[3,4]

Acknowledgements

We thank Pieter Roelfsema for enabling the collaboration that led to the access to the patients, Eline Ramaaker for her assistance in electrode localization, Agneta Fischer and

George Bulte at UvA for advice and help with the use of FaceReader, and Tess den Uyl for advice on how to use FaceReader specifically to analyse facial expressions of pain.

Funding

This work was supported by Dutch Research Council (NWO) VIDI grant (452-14-015) to VG and VICI grant (453-15-009) to CK.

Competing interests

The authors report no competing interests.

Supplementary material

Supplementary material is available at biorxiv.org.

References

1. Lamm C, Decety J, Singer T. Meta-analytic evidence for common and distinct neural networks associated with directly experienced pain and empathy for pain. *NeuroImage*. 2011;54(3):2492-2502. doi:10.1016/j.neuroimage.2010.10.014
2. Keysers C, Kaas JH, Gazzola V. Somatosensation in social perception. *Nat Rev Neurosci*. 2010;11(6):417-428. doi:10.1038/nrn2833
3. Timmers I, Park AL, Fischer MD, et al. Is Empathy for Pain Unique in Its Neural Correlates? A Meta-Analysis of Neuroimaging Studies of Empathy. *Front Behav Neurosci*. 2018;12. doi:10.3389/fnbeh.2018.00289
4. Jauniaux J, Khatibi A, Rainville P, Jackson PL. A meta-analysis of neuroimaging studies on pain empathy: investigating the role of visual information and observers' perspective. *Soc Cogn Affect Neurosci*. 2019;14(8):789-813. doi:10.1093/scan/nsz055
5. Paradiso E, Gazzola V, Keysers C. Neural mechanisms necessary for empathy-related phenomena across species. *Curr Opin Neurobiol*. Published online 2021. doi:10.1016/j.conb.2021.02.005
6. Hutchison WD, Davis KD, Lozano AM, Tasker RR, Dostrovsky JO. Pain-related neurons in the human cingulate cortex. *Nat Neurosci*. 1999;2(5):403-405. doi:10.1038/8065
7. Carrillo M, Han Y, Migliorati F, Liu M, Gazzola V, Keysers C. Emotional Mirror Neurons in the Rat's Anterior Cingulate Cortex. *Curr Biol*. 2019;29(8):1301-1312.e6. doi:10.1016/j.cub.2019.03.024
8. Wicker B, Keysers C, Plailly J, Royet JP, Gallese V, Rizzolatti G. Both of us disgusted in My insula: the common neural basis of seeing and feeling disgust. *Neuron*. 2003;40(3):655-664.
9. Singer T, Seymour B, O'Doherty J, Kaube H, Dolan RJ, Frith CD. Empathy for pain involves the affective but not sensory components of pain. *Science*. 2004;303(5661):1157-1162. doi:10.1126/science.1093535
10. Jabbi M, Swart M, Keysers C. Empathy for positive and negative emotions in the gustatory cortex. *NeuroImage*. 2007;34(4):1744-1753. doi:10.1016/j.neuroimage.2006.10.032

11. Meffert H, Gazzola V, den Boer JA, Bartels AAJ, Keysers C. Reduced spontaneous but relatively normal deliberate vicarious representations in psychopathy. *Brain J Neurol*. 2013;136(Pt 8):2550-2562. doi:10.1093/brain/awt190
12. Liberati G, Mulders D, Algoet M, et al. Insular responses to transient painful and non-painful thermal and mechanical spinothalamic stimuli recorded using intracerebral EEG. *Sci Rep*. 2020;10(1):22319. doi:10.1038/s41598-020-79371-2
13. Jobst BC, Gonzalez-Martinez J, Isnard J, et al. The Insula and Its Epilepsies. *Epilepsy Curr*. 2019;19(1):11-21. doi:10.1177/1535759718822847
14. Mazzola L, Isnard J, Peyron R, Mauguière F. Stimulation of the human cortex and the experience of pain: Wilder Penfield's observations revisited. *Brain J Neurol*. 2012;135(Pt 2):631-640. doi:10.1093/brain/awr265
15. Adolphs R, Tranel D, Damasio AR. Dissociable neural systems for recognizing emotions. *Brain Cogn*. 2003;52(1):61-69. doi:10.1016/S0278-2626(03)00009-5
16. Zinchenko O, Yaple ZA, Arsalidou M. Brain Responses to Dynamic Facial Expressions: A Normative Meta-Analysis. *Front Hum Neurosci*. 2018;12:227. doi:10.3389/fnhum.2018.00227
17. Gallo S, Paracampo R, Müller-Pinzler L, et al. The causal role of the somatosensory cortex in prosocial behaviour. *eLife*. 2018;7. doi:10.7554/eLife.32740
18. Adolphs R, Damasio H, Tranel D, Cooper G, Damasio AR. A role for somatosensory cortices in the visual recognition of emotion as revealed by three-dimensional lesion mapping. *J Neurosci*. 2000;20(7):2683-2690. doi:10.1523/jneurosci.20-07-02683.2000
19. Dal Monte O, Krueger F, Solomon JM, et al. A voxel-based lesion study on facial emotion recognition after penetrating brain injury. *Soc Cogn Affect Neurosci*. 2013;8(6):632-639. doi:10.1093/scan/nss041
20. Mattavelli G, Pisoni A, Casarotti A, et al. Consequences of brain tumour resection on emotion recognition. *J Neuropsychol*. 2019;13(1):1-21. doi:https://doi.org/10.1111/jnp.12130
21. Fried I, Wilson CL, Maidment NT, et al. Cerebral microdialysis combined with single-neuron and electroencephalographic recording in neurosurgical patients. Technical note. *J Neurosurg*. 1999;91(4):697-705. doi:10.3171/jns.1999.91.4.0697
22. Keysers C, Gazzola V, Wagenmakers E-J. Using Bayes factor hypothesis testing in neuroscience to establish evidence of absence. *Nat Neurosci*. 2020;23(7):788-799. doi:10.1038/s41593-020-0660-4
23. Quiroga RQ, Nadasdy Z, Ben-Shaul Y. Unsupervised Spike Detection and Sorting with Wavelets and Superparamagnetic Clustering. *Neural Comput*. 2004;16(8):1661-1687. doi:10.1162/089976604774201631
24. Bartoli E, Bosking W, Chen Y, et al. Functionally Distinct Gamma Range Activity Revealed by Stimulus Tuning in Human Visual Cortex. *Curr Biol CB*. 2019;29(20):3345-3358.e7. doi:10.1016/j.cub.2019.08.004
25. Buzsáki G, Anastassiou CA, Koch C. The origin of extracellular fields and currents--EEG, ECoG, LFP and spikes. *Nat Rev Neurosci*. 2012;13(6):407-420. doi:10.1038/nrn3241
26. Miller KJ, Honey CJ, Hermes D, Rao RPN, denNijs M, Ojemann JG. Broadband changes in the cortical surface potential track activation of functionally diverse neuronal populations. *NeuroImage*. 2014;85 Pt 2:711-720. doi:10.1016/j.neuroimage.2013.08.070
27. Kunz M, Meixner D, Lautenbacher S. Facial muscle movements encoding pain-a systematic review. *Pain*. 2019;160(3):535-549. doi:10.1097/j.pain.0000000000001424
28. Jeffreys H. *Theory of Probability*. 2nd ed. Oxford University Press; 1939.
29. Ingvar M. Pain and functional imaging. Howseman A, Zeki S, eds. *Philos Trans R Soc Lond B Biol Sci*. 1999;354(1387):1347-1358. doi:10.1098/rstb.1999.0483

30. Bernhardt BC, Singer T. The Neural Basis of Empathy. *Annu Rev Neurosci*. 2012;35(1):1-23. doi:10.1146/annurev-neuro-062111-150536
31. Zaki J, Wager TD, Singer T, Keysers C, Gazzola V. The Anatomy of Suffering: Understanding the Relationship between Nociceptive and Empathic Pain. *Trends Cogn Sci*. 2016;20(4):249-259. doi:10.1016/j.tics.2016.02.003
32. Uddin LQ. Salience processing and insular cortical function and dysfunction. *Nat Rev Neurosci*. 2015;16(1):55-61. doi:10.1038/nrn3857
33. Legrain V, Iannetti GD, Plaghki L, Mouraux A. The pain matrix reloaded: A salience detection system for the body. *Prog Neurobiol*. 2011;93(1):111-124. doi:10.1016/j.pneurobio.2010.10.005
34. Krolak-Salmon P, Hénaff M-A, Isnard J, et al. An attention modulated response to disgust in human ventral anterior insula. *Ann Neurol*. 2003;53(4):446-453. doi:10.1002/ana.10502
35. Chen Y-H, Dammers J, Boers F, et al. The temporal dynamics of insula activity to disgust and happy facial expressions: a magnetoencephalography study. *NeuroImage*. 2009;47(4):1921-1928. doi:10.1016/j.neuroimage.2009.04.093
36. Zhou F, Li J, Zhao W, et al. Empathic pain evoked by sensory and emotional-communicative cues share common and process-specific neural representations. Shackman A, Büchel C, Mehta M, Vatansever D, eds. *eLife*. 2020;9:e56929. doi:10.7554/eLife.56929
37. Tovote P, Fadok JP, Lüthi A. Neuronal circuits for fear and anxiety. *Nat Rev Neurosci*. 2015;16(6):317-331. doi:10.1038/nrn3945
38. Likhtik E, Stujenske JM, Topiwala MA, Harris AZ, Gordon JA. Prefrontal entrainment of amygdala activity signals safety in learned fear and innate anxiety. *Nat Neurosci*. 2014;17(1):106-113. doi:10.1038/nn.3582
39. Taub AH, Perets R, Kahana E, Paz R. Oscillations Synchronize Amygdala-to-Prefrontal Primate Circuits during Aversive Learning. *Neuron*. 2018;97(2):291-298.e3. doi:10.1016/j.neuron.2017.11.042
40. Gazzola V, Keysers C. The Observation and Execution of Actions Share Motor and Somatosensory Voxels in all Tested Subjects: Single-Subject Analyses of Unsmoothed fMRI Data. *Cereb Cortex*. 2009;19(6):1239-1255. doi:10.1093/cercor/bhn181
41. Caspers S, Zilles K, Laird AR, Eickhoff SB. ALE meta-analysis of action observation and imitation in the human brain. *NeuroImage*. 2010;50(3):1148-1167. doi:10.1016/j.neuroimage.2009.12.112
42. Abdelgabar AR, Suttrup J, Broersen R, et al. Action perception recruits the cerebellum and is impaired in patients with spinocerebellar ataxia. *Brain*. 2019;142(12):3791-3805. doi:10.1093/brain/awz337
43. Pobric G, de C. Hamilton AF. Action Understanding Requires the Left Inferior Frontal Cortex. *Curr Biol*. 2006;16(5):524-529. doi:10.1016/j.cub.2006.01.033
44. Keysers C, Paracampo R, Gazzola V. What neuromodulation and lesion studies tell us about the function of the mirror neuron system and embodied cognition. *Curr Opin Psychol*. 2018;24:35-40. doi:10.1016/j.copsyc.2018.04.001
45. Maris E, Oostenveld R. Nonparametric statistical testing of EEG- and MEG-data. *J Neurosci Methods*. 2007;164(1):177-190. doi:10.1016/j.jneumeth.2007.03.024